

## CCD SURFACE PHOTOMETRY OF SPIRAL GALAXIES: BULGE MORPHOLOGY

HONG BAE ANN

Department of Earth Sciences, Pusan National University, Busan 609-735, Korea

*E-mail: hbann@cosmos.es.pusan.ac.kr*

*(Received September 17, 2003; Accepted October 21, 2003)*

### ABSTRACT

We have conducted a  $V$ -band CCD surface photometry of 68 disk galaxies to analyze the bulge morphology of nearby spirals. We classify bulges into four types according to their ellipticities and the misalignments between the major axis of the bulge and those of the disk and the bar: spherical, oblate, pseudo triaxial, and triaxial. We found that one third of the bulges are triaxial and they are preponderant in barred galaxies. The presence of the triaxial bulges in a significant fraction of unbarred galaxies as well as in barred galaxies might support the secular evolution hypothesis which postulates that the bar driven mass inflow leads to the formation of triaxial bulges and the destruction of bars when sufficient mass is accumulated in the central regions.

*Key words* : galaxies: spiral - galaxies: structure - galaxies: bulge - galaxies: surface photometry

### I. INTRODUCTION

Spiral galaxies consist of distinct building blocks; disk, bulge, and dark halo. The Hubble sequence is basically a sequence of the disk-to-bulge ratio which can be estimated by the surface photometry of galaxies. Until recently, the bulges are thought to be featureless like scale-downed ellipticals whose luminosity distribution is well described by the  $r^{1/4}$ -law. Their morphology is supposed to be maintained since their formation. But, recent ground based and *HST* images of a sample of spiral galaxies show that a significant fraction of spiral bulges display a variety of nuclear features such as nuclear rings, nuclear spirals, and nuclear bars (Mulchaey, Regan & Kundu 1997; Regan & Mulchaey 1999; Martini & Pogge 1999; Martini et al.2003). Moreover, some of bulges are known to be disky (Kormendy 1993; Andredakis, Peletier & Balcells 1995; Courteau, de Jong & Broeils 1996; Carollo et al.1997). Since these nuclear features are supposed to be transient ones, we may expect an ongoing secular evolution which can transform the bulge morphology.

In the classical picture of galaxy formation, incorporated with the hierarchical clustering and dissipation scenario (e.g., White & Rees 1978), the bulge forms first from the collapse of proto-galactic clouds which are embedded in the dark halo, while the disk forms from the in-falling material after the bulge forms. Basically the same picture is maintained in recent theoretical and dynamical models (van den Bosch 1998; Elmegreen 1999; Samland & Gerhard 2003). However, there are several alternative scenarios in which the bulge forms after the disk, by merger events (Kauffmann, White & Guiderdoni 1993; Baugh, Cole and Frenk 1996) or by secular evolution driven by the bar (Friedli & Benz 1993, 1995) or driven by the dynamical friction in the young clumpy disks (Noguchi 1999, 2000).

There are several observational and theoretical evidences for the secular evolution of galaxies which lead to the transformation of bulge morphology within the Hubble time (Pfenniger & Norman 1990; Friedli & Martinet 1993; Courteau, de Jong & Broeils 1996; Zhang 1996, 1998). The triaxial bulges and peanut/box shaped bulges are thought to be the result of secular evolution driven mostly by the bars (Pfenniger & Norman 1990; Friedli & Benz 1993, 1995). A good example of triaxial bulges which might be caused by secular evolution is the bulge of NGC 4314, which is characterized by the isophotal twists caused by nuclear spirals and dust lanes (Benedict et al.1992, 1996; Ann 2001).

An analysis of bulge morphology of barred galaxies using Kiso Schmidt plates (Ann 1995) showed that more than half of the bulges of barred galaxies is triaxial. If the triaxial bulges are made by secular evolution, we expect that they are more preponderant in barred galaxies than in unbarred galaxies. The purpose of the present study is to draw some insights on the origin of triaxial bulges by analyzing the frequency distribution of bulge types. To do this, we have conducted CCD surface photometry of 68 spiral galaxies in  $V$ -band which is thought to be an ideal passband for morphological studies because it allows an easy comparison with the previous photometry and is less affected by the dust extinction than  $B$ -band.

In this paper we present a brief analysis of the bulge morphology of 68 disk galaxies based on the  $V$ -band images. More detailed analysis of luminosity distribution of the observed galaxies, including the statistics of the bulge-to-disk ratios will be given elsewhere. In §2, we describe the observation and data reduction. The isophotal maps of 68 spiral galaxies are presented in §3, and discussion on the origin of the triaxial bulges is presented in §4. The conclusion of the present study is

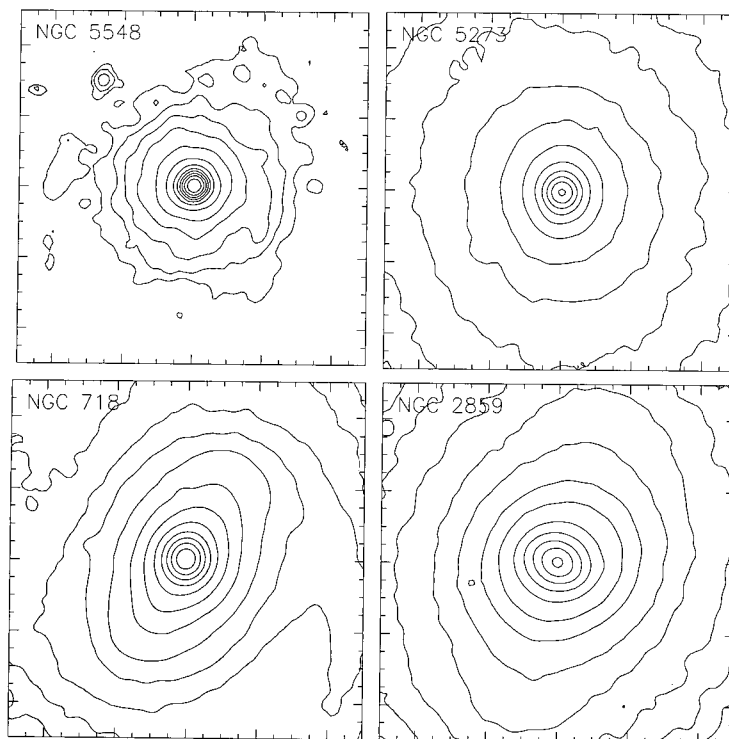


Fig. 1.— Isophotal maps of the four proto type galaxies, NGC 0718 (T'), NGC 2859 (T), NGC 5273 (O), and NGC 5548 (S). The size of each box is  $68'' \times 68''$ . North is up and east to the left.

given in the last section.

## II. OBSERVATIONS AND REDUCTIONS

CCD images of 68 bright disk galaxies in  $V$  passband are obtained by the BOAO 1.8m telescope during the observing runs from 1997 January to 1998 November. We used a  $1024 \times 1024$  Tek CCD whose field of view is  $5.8''$  in earlier observing runs, but we replaced it with  $2048 \times 2048$  Tek CCD whose field of view is twice of the previous one after 1997 May. The seeing was between  $1.2''$  and  $2.5''$ . The exposure times of target galaxies varied between 200 sec and 600 sec depending on the galaxy brightness and the sky conditions. We obtained a sufficient number of bias frames at the beginning and end of the nights and derived a mean bias frame for each night. We observed the evening and morning twilight sky for flat-fielding. We obtained more than ten twilight sky frames per night. Dark frames were also obtained during the observing runs but it was found to be negligible for the adopted exposure times. We observed a number of standard stars (Landolt 1992) during the nights for the standardization of the photometry.

We have followed a standard procedure of CCD reduction by using the *ccdred* package in IRAF. It includes trimming, bias subtraction, overscan correction, and flat-fielding. We used a mean bias frame of each

night for bias subtraction and a master flat-field of each observing run for flat-fielding. The master flat-fields were derived by combining twilight sky frames of which signal-to-noise ratio is larger than 100.

The flat-fielded frames of galaxy images were subtracted and divided by the sky frames, which were obtained by fitting the sky regions surrounding the galaxy images, to obtain the galaxy light distribution expressed in unit of local sky level as

$$I_{rel}(x, y) = \frac{I_{G+S}(x, y) - I_S(x, y)}{I_S(x, y)},$$

where  $I_{G+S}(x, y)$  is the measured intensity from the galaxy and the sky, and  $I_S(x, y)$  is the background local sky intensity, respectively. To do this, we used SPIRAL package developed for the surface photometry of galaxies at Kiso observatory (Ichikawa et al.1987).

The galaxy images were trimmed and registered so that the center of a galaxy is located at the center of the image. The registered galaxy images were smoothed to increase the signal-to-noise ratios using variable beam Gaussian smoothing which makes heavy smoothing for the outer part of the galaxy and light smoothing for the bright inner part. The foreground and background stars were cleaned from the smoothed images for further analyses. Because the galaxy light distribution is expressed in unit of the local sky intensity, the distribu-

tion of the surface brightness of a galaxy is determined by the sky brightness  $\mu_{sky}$  as

$$\mu(x, y) = -2.5 \log I_{rel}(x, y) + \mu_{sky}.$$

The sky brightness  $\mu_{sky}$  is determined by aperture photometry of the Landolt (1992) standard stars observed during the observations.

### III. RESULTS

#### (a) Morphology of Spiral Bulges

The bulges of spiral galaxies can be classified into four types according to their ellipticities and position angles relative to the disks and bars (Ann 1995): spherical bulge (S), oblate bulge (O), pseudo triaxial bulge (T'), and triaxial bulge (T). The ellipticities and position angles of the galaxies were determined by fitting concentric ellipses to the observed isophotes. In the case of barred galaxies the position angles of bars were also taken into account. We have assigned the bulges with  $\epsilon \leq 0.1$  to S and those with  $\epsilon > 0.1$  to T. But, among the bulges with  $\epsilon > 0.1$ , we classified them as O if the bulge-disk misalignment ( $\Delta PA_{bulge-disk}$ ) is larger than  $10^\circ$ , whereas we classified them as T' if the bulge-bar misalignment ( $\Delta PA_{bulge-bar}$ ) is less than  $10^\circ$ . Fig. 1 shows the prototype morphology of each bulge type; NGC 5548 (S), NGC 5273 (O), NGC 718 (T'), and NGC 2859 (T). The outer most isophotes are  $3.5 \text{ mag/arcsec}^2$  below the sky level and the intervals of the isophotes are  $0.5 \text{ mag/arcsec}^2$  each.

Fig. 2 shows the V-band isophotal maps of the 68 spiral galaxies. Because we are mainly interested in the bulge morphology of the nearby spiral galaxies, the size of the isophotal maps is chosen to be  $34'' \times 34''$  which is large enough to display the bulge components of the nearest galaxies in our sample. It is apparent that the bulges of disk galaxies have various shapes, from spheres to highly elongated ones. In Table 1, we present the bulge types and the geometrical parameters of 68 galaxies from the ellipse fitting. As shown in Table 1, the geometrical parameters of bulges are not much affected by the atmospheric seeing since we derived the bulge parameter at the radii outside the seeing disk for most of the galaxies.

#### (b) Frequency Distribution of Triaxial Bulges

Fig. 3 shows the frequency distribution of the bulge types of the present sample of galaxies. The fraction of spherical bulges is largest for the unbarred disk galaxies, while that of triaxial bulges is greatest for the barred galaxies. The distribution of bulge types in the transition type galaxies is somewhat similar to that of the unbarred galaxies. The fraction of triaxial bulges in barred galaxies is about 40%. But, if we consider that half of the pseudo triaxial bulges are genuine triaxial bulges whose major axes are happen to lie close to the bar axes, more than half of the bulges in barred

galaxies are triaxial. Although the number of galaxies in the present sample is not large enough to draw a firm conclusion on the frequency distribution of triaxial bulges, our finding is in good agreement with the earlier studies (Varela, Simonneau, & Munoz-Tunon 1993; Ann 1995; Shaw et al. 1995) which showed that triaxial bulges are more preponderate in barred galaxies. As shown in Fig. 3, however, the triaxial bulges are also very common in unbarred galaxies. In total, about one third of the spiral bulges is triaxial.

It is of worth to note that the triaxial bulges are most frequently observed in galaxies with intermediate Hubble types where strong bars are likely to be found (Ann & Lee 1987; Elmegreen & Elmegreen 1985). Fig. 4 shows the distribution of bulge ellipticity along the Hubble type where open and filled circles represent the spherical and oblate bulges, respectively, whereas open and filled triangles indicate the pseudo triaxial and triaxial bulges, respectively. Among 11 galaxies that have Hubble types Sb or SBb 6 galaxies have triaxial bulges. The high fraction of triaxial bulges in barred galaxies, especially in strongly barred galaxies, may support the secular evolution hypothesis that triaxial bulges of barred galaxies are made from the inflowing disk material driven by the bar (Kormendy 1979) since strong bars are known to be effective to drive the gas inflow toward the galactic nuclei (Ann & Lee 2000).

### IV. DISCUSSION

#### (a) Origin of Triaxial Bulges

As shown in Fig. 3, about a half of the bulges of barred galaxies and about one third of the bulges in unbarred galaxies are triaxial. The preponderance of the triaxial bulges in barred galaxies can be understood in terms of the secular evolution driven by the bar (Kormendy 1979; Pfenninger & Norman 1990; Friedli and Benz 1993, 1995). For the transition type galaxies, the same mechanism can be responsible for the formation of triaxial bulges because there is non-axisymmetric potential, similar to that of the bar.

For unbarred galaxies, spiral arms do play the same role as the bars. They can redistribute angular momentum of the disk, which yields the transportation of disk material into the galactic nuclei. One of the probable mechanisms for the angular momentum redistribution in unbarred spirals is the phase shift proposed by Zhang (1996). However, spiral arms seem to be less effective than the bars in transporting disk material into the nuclear region of galaxies because the gravitational torque of the spiral arms is weaker than that of the bar. Thus, it is unclear whether the secular evolution driven by the spiral arms is rapid enough to transform the spherical bulges into the triaxial ones. We need detailed simulations for the formation and evolution of bulges in unbarred spiral galaxies to clarify this problem.

An alternative idea for the triaxial bulges in unbarred galaxies is that they are nothing but the de-

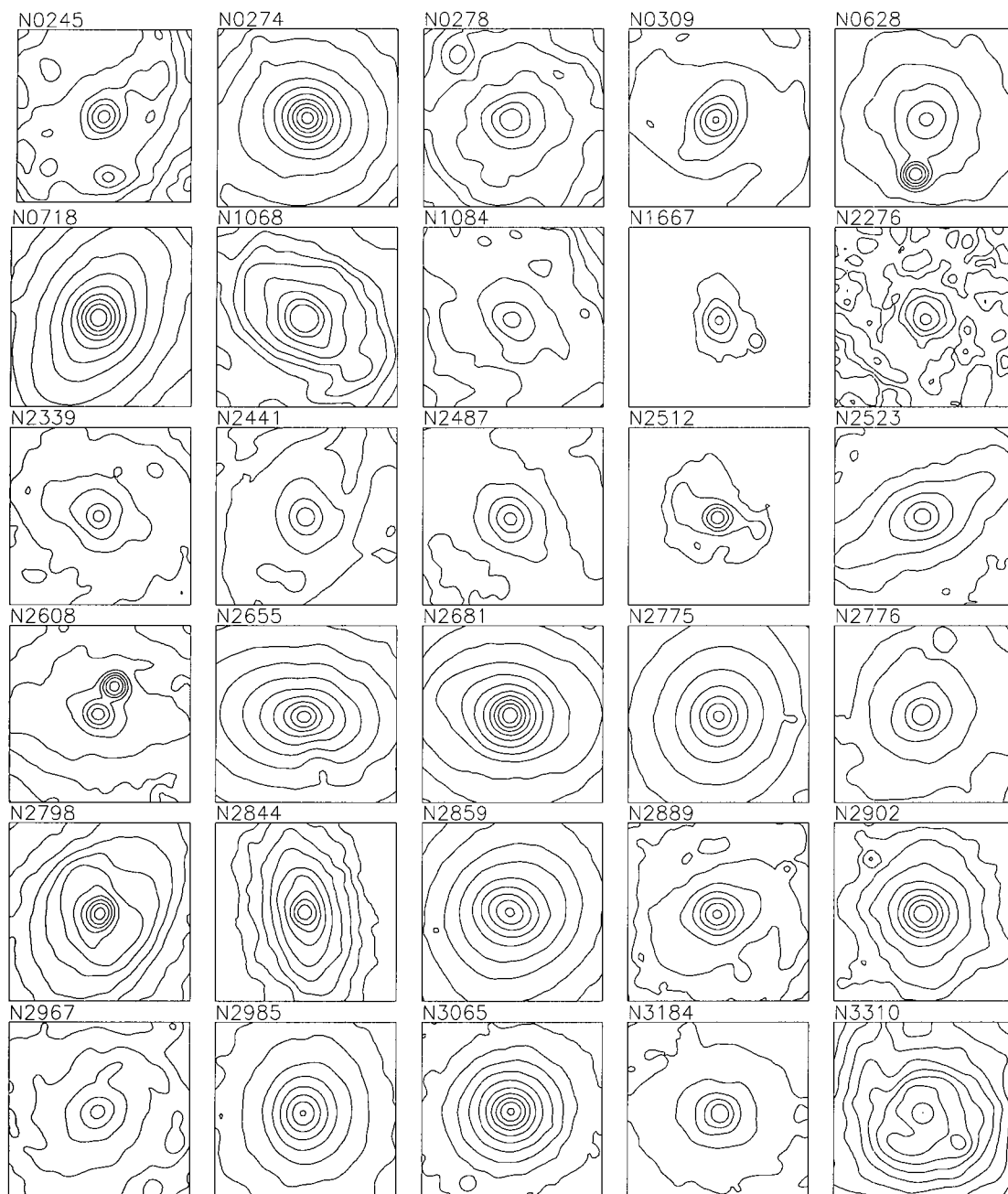


**Fig. 2.**— Isophotal maps of 68 galaxies. The size of each box is  $34'' \times 34''$ . The interval of isophotes is  $0.5 \text{ mag/arcsec}^2$ . North is up and east to the left.

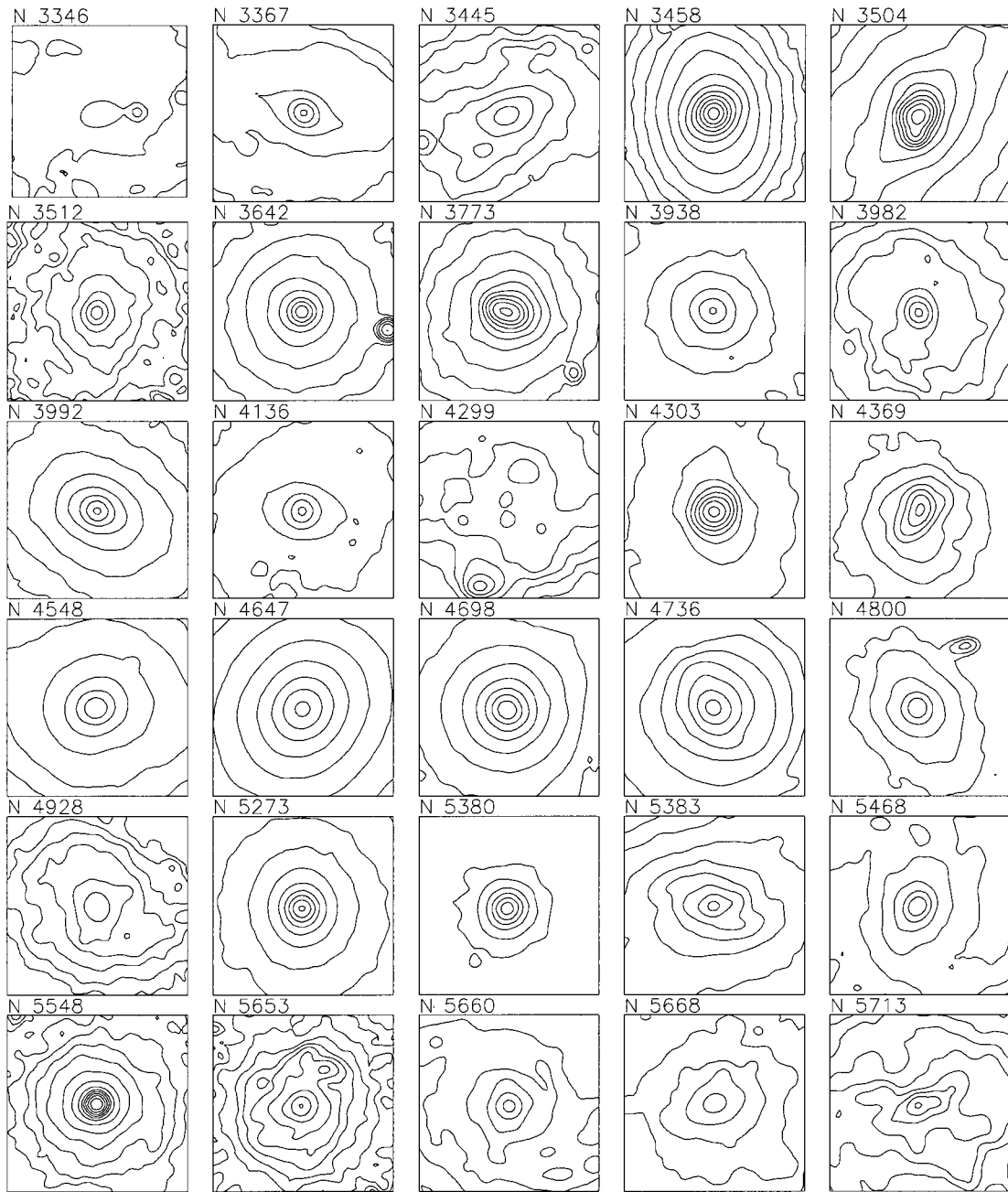


Fig. 2.— - continued -

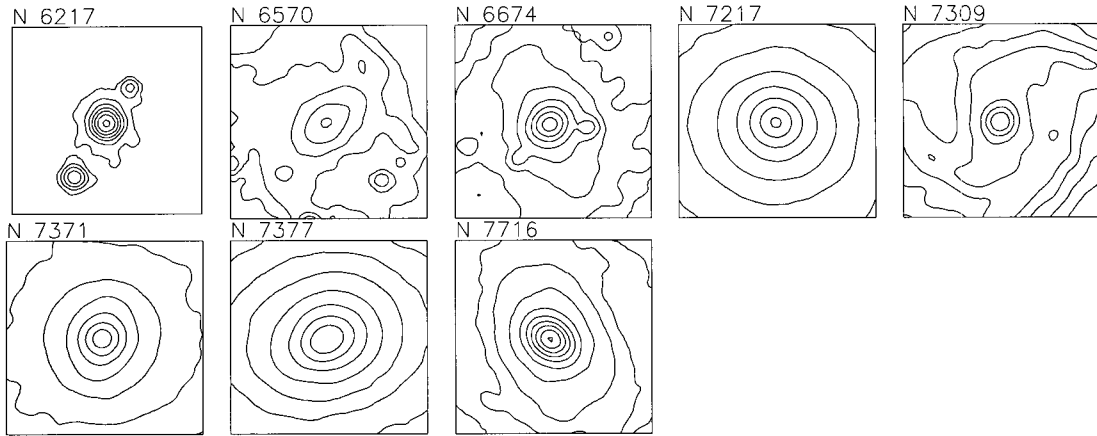


Fig. 2.— - continued -

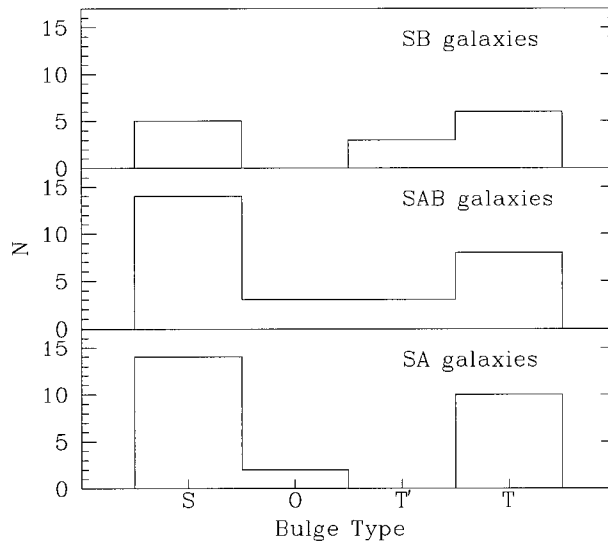


Fig. 3.— Frequency distribution of bulge types. The bulge type S and O denote the spherical and oblate bulges, respectively, while T' and T represent the pseudo triaxial and triaxial bulges. See the text for the description of the bulge types.

TABLE 1  
BASIC PARAMETERS AND BULGE TYPES

| Galaxy   | Type                   | Dia( $l$ ) | V(km/s) | $\epsilon_{bg}$ | Bulge |
|----------|------------------------|------------|---------|-----------------|-------|
| NGC 0245 | SA(rs)b                | 1.4x1.2    | 4060    | 0.13            | T     |
| NGC 0274 | SAB(r)0 <sup>-</sup>   | 1.5x1.5    | 1750    | 0.09            | S     |
| NGC 0278 | SAB(rs)b               | 2.1x2.0    | 640     | 0.13            | T     |
| NGC 0309 | SAB(r)c                | 3.0x2.5    | 5662    | 0.04            | S     |
| NGC 0628 | SA(s)c                 | 10.5x9.5   | 657     | 0.05            | S     |
| NGC 0718 | SAB(s)a                | 2.3x2.0    | 1733    | 0.13            | T'    |
| NGC 1068 | (R)SA(rs)b             | 7.1x6.0    | 1137    | 0.11            | T     |
| NGC 1084 | SA(s)c                 | 3.2x1.8    | 1406    | 0.12            | T     |
| NGC 1667 | SAB(r)c                | 1.8x1.4    | 4547    | 0.12            | O     |
| NGC 2276 | SAB(rs)c               | 2.8x2.7    | 2410    | 0.02            | S     |
| NGC 2339 | SAB(rs)bc              | 2.7x2.0    | 2206    | 0.09            | S     |
| NGC 2441 | SAB(r)b                | 2.0x1.7    | 3470    | 0.05            | S     |
| NGC 2487 | SB(r)c                 | 2.6x2.1    | 4841    | 0.06            | S     |
| NGC 2512 | SBb                    | 1.4x0.9    | 4702    | 0.27            | T     |
| NGC 2523 | SB(s)c                 | 1.0x0.7    | 3804    | 0.19            | T'    |
| NGC 2608 | SB(s)b                 | 2.3x1.4    | 2135    | 0.01            | S     |
| NGC 2655 | SAB(s)0/a              | 4.9x4.1    | 1404    | 0.27            | T'    |
| NGC 2681 | (R')SAB(rs)0/a         | 3.6x3.3    | 692     | 0.09            | S     |
| NGC 2775 | SA(r)ab                | 4.3x3.3    | 1354    | 0.10            | S     |
| NGC 2776 | SAB(rs)c               | 3.0x2.7    | 2626    | 0.07            | S     |
| NGC 2798 | SB(s)a                 | 2.6x1.0    | 1726    | 0.25            | T     |
| NGC 2844 | SA(r)a                 | 1.5x0.8    | 1486    | 0.34            | O     |
| NGC 2859 | (R)SB(r)0 <sup>+</sup> | 4.3x3.8    | 1687    | 0.14            | T     |
| NGC 2889 | SAB(rs)c               | 2.2x1.9    | 3337    | 0.04            | S     |
| NGC 2902 | SA(s)0 <sup>0</sup>    | 1.4x1.2    | 1990    | 0.02            | S     |
| NGC 2967 | SA(s)c                 | 3.0x2.8    | 1892    | 0.09            | S     |
| NGC 2985 | (R')SA(rs)ab           | 4.6x3.6    | 1322    | 0.13            | T'    |
| NGC 3065 | SA(r)0 <sup>0</sup>    | 1.7x1.7    | 2000    | 0.02            | S     |
| NGC 3184 | SAB(rs)cd              | 7.4x6.9    | 592     | 0.04            | S     |
| NGC 3310 | SAB(r)bc               | 3.1x2.4    | 993     | 0.06            | S     |
| NGC 3346 | SB(rs)cd               | 2.9x2.5    | 1260    | 0.35            | T'    |
| NGC 3367 | SB(rs)c                | 2.5x2.2    | 3037    | 0.15            | T     |
| NGC 3445 | SAB(s)m                | 1.6x1.5    | 2069    | 0.15            | O     |
| NGC 3458 | SAB                    | 1.4x0.9    | 1818    | 0.12            | T     |
| NGC 3504 | (R)SAB(s)ab            | 2.7x2.1    | 1534    | 0.30            | T     |
| NGC 3512 | SAB(rs)c               | 1.6x1.5    | 1376    | 0.12            | O     |
| NGC 3642 | SA(r)bc                | 5.4x4.5    | 1588    | 0.02            | S     |
| NGC 3773 | SA0                    | 1.2x1.0    | 987     | 0.08            | S     |
| NGC 3938 | SA(s)c                 | 5.4x4.9    | 809     | 0.08            | S     |
| NGC 3982 | SAB(r)b                | 2.3x2.0    | 1109    | 0.16            | T     |
| NGC 3992 | SB(rs)bc               | 7.6x4.7    | 1048    | 0.20            | T     |
| NGC 4136 | SAB(r)c                | 4.0x3.7    | 609     | 0.16            | T     |
| NGC 4299 | SAB(s)dm               | 1.7x1.6    | 232     | 0.44            | T     |
| NGC 4303 | SAB(rs)bc              | 6.5x5.8    | 1566    | 0.04            | S     |
| NGC 4369 | (R)SA(rs)a             | 2.1x2.0    | 1045    | 0.39            | T     |
| NGC 4548 | SBb(rs)                | 5.4x4.3    | 486     | 0.08            | S     |
| NGC 4647 | SAB(rs)c               | 2.9x2.3    | 1422    | 0.05            | S     |
| NGC 4698 | SA(s)ab                | 4.0x2.5    | 1002    | 0.03            | S     |
| NGC 4736 | (R)SA(r)ab             | 11.2x9.1   | 308     | 0.11            | T     |
| NGC 4800 | SA(rs)b                | 1.6x1.2    | 891     | 0.10            | S     |
| NGC 4928 | SA(s)bc                | 1.3x1.0    | 1720    | 0.17            | T     |
| NGC 5273 | SA(s)0 <sup>0</sup>    | 2.8x2.5    | 1064    | 0.12            | O     |

TABLE 1  
 - CONTINUED

| Galaxy   | Type                | Dia( $l$ ) | V(km/s) | $\epsilon_{bg}$ | Bulge |
|----------|---------------------|------------|---------|-----------------|-------|
| NGC 5380 | SA0 <sup>-</sup>    | 1.7x1.7    | 3173    | 0.06            | S     |
| NGC 5383 | (R')SB(rs)b         | 3.2x2.7    | 2270    | 0.56            | T     |
| NGC 5468 | SAB(rs)cd           | 2.6x2.4    | 2845    | 0.19            | T     |
| NGC 5548 | (R')SA(s)0/a        | 1.4x1.3    | 5149    | 0.05            | S     |
| NGC 5653 | (R')SA(rs)b         | 1.7x1.3    | 3562    | 0.08            | S     |
| NGC 5660 | SAB(rs)c            | 2.8x2.5    | 2328    | 0.06            | S     |
| NGC 5668 | SA(s)d              | 3.3x3.0    | 1583    | 0.11            | T     |
| NGC 5713 | SAB(rs)bc           | 2.8x2.5    | 1972    | 0.47            | T'    |
| NGC 6217 | (R)SB(rs)bc         | 3.0x2.5    | 1362    | 0.08            | S     |
| NGC 6570 | SB(rs)m             | 1.8x1.1    | 2281    | 0.13            | T'    |
| NGC 6674 | SB(r)b              | 4.0x2.2    | 3429    | 0.10            | S     |
| NGC 7217 | (R)SA(r)ab          | 3.9x3.2    | 952     | 0.06            | S     |
| NGC 7309 | SAB(rs)c            | 1.9x1.8    | 4005    | 0.09            | S     |
| NGC 7371 | (R)SA(r)0/a         | 2.0x2.0    | 2685    | 0.16            | T     |
| NGC 7377 | SA(s)0 <sup>+</sup> | 3.0x2.5    | 3351    | 0.17            | T     |
| NGC 7716 | SAB(r)b             | 2.1x1.8    | 2571    | 0.18            | T     |

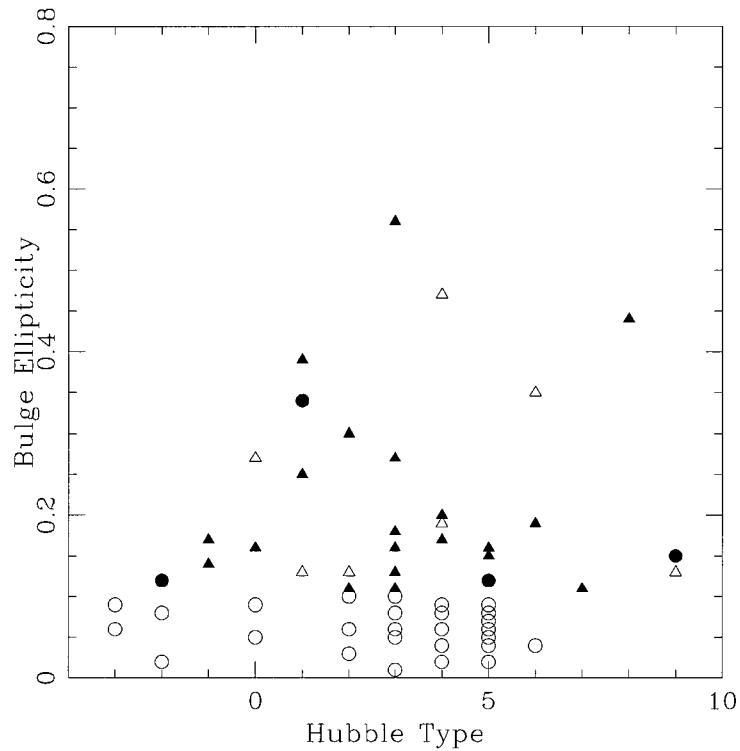


Fig. 4.— Bulge ellipticities and the Hubble types. Open circle, closed circle, open triangle and closed triangle represent the bulge types of S, O, T', and T, respectively.



stroyed bars. Since bars are prone to be destroyed by the high central mass concentration (Norman, Sellwood, & Hassan 1996; Das et al 2003), the accumulation of mass in the central region due to the bar forcing leads to the destruction of the bar itself. However, this scenario can be applied only to the triaxial bulges of early type spiral galaxies because mass accumulation in the central region driven by the bar transforms the late type bulges into earlier ones before the destruction of the bar. In this picture of secular evolution, there is a duty cycle of the bar which drives the evolution of galaxies in the Hubble time .

Of course, it seems to be plausible that the triaxial bulges are the consequences of the multiple mergers during the early period of galaxy formation. However, it is difficult to analyze the bulge morphology from the hierarchical clustering models for the structure formation due to the lack of numerical resolution (e.g., Navarro, Frenk, & White 1995 and references therein). Recent hydrodynamic simulations in the framework of CDM cosmology which provide high enough resolution to investigate the shape of galactic bulges show realistic bulges following de Vaucouleur  $r^{1/4}$  law but their bulges appear to be spherical ones (Gnedin, Norman & Ostriker 2000).

### (b) Nuclear Features

High resolution *HST* images of nearby normal spirals (Phillips et al.1996) and active galaxies (Regan & Mulchaey 1999; Martini & Pogge 1999; Pogge & Martini 2002) showed that the bulges of spiral galaxies display nuclear features such as nuclear rings, nuclear spirals, and nuclear bars. Some of the galaxies in the present sample are found to have such features: e.g., nuclear spirals in NGC 5383 (Martini et al.2003). These nuclear features can not be resolved by the ground-based observations such as ours because most of the features are confined to the inner kpc of the galactic nuclei. However, our analysis of bulge morphology seems to be not much affected by the presence of these features because we classify the bulge morphology not by the isophotal twists in the nuclear regions but by the misalignment between the bulge and the disk. The isophotal twists that represent the variation of the position angles of the major axis along the radius is known to be a direct evidence of the triaxiality (Stark 1977), but it can be affected by the irregular dust extinction. Of course, position angles of the bulges can be affected by the dust extinction, however, our measure of the bulge position angle is not much affected by the nuclear dustlanes since they are located in the inner kpc regions while we measure the bulge position angle outside these regions for most of the galaxies.

## V. CONCLUSIONS

We have analyzed the bulge morphology of 68 spiral galaxies based on the *V*-band CCD surface photome-

try conducted at BOAO. The nuclear features such as nuclear rings, nuclear spirals, and nuclear bars, which are known to be present in some of the present sample, are not resolved in the present observations due to the lack of resolution. However, our analysis of the bulge morphology is not much affected by the unresolved nuclear features because we classify bulge type not by the isophotal twist in the nuclear regions but by the misalignment between the bulge and the disk. Moreover, most of the features are confined to the inner kpc of the galactic nuclei, while most of spiral bulges extend far beyond these regions. Thus, the isophotal maps from the present photometry seem to be good enough to analyze the bulge morphology.

The triaxial bulges are found to be preponderant not only in barred galaxies but also in unbarred galaxies. In average, about one third of the spiral bulges are triaxial with the highest fraction of triaxial bulges ( $\sim 50\%$ ) in barred galaxies. The high frequency of the triaxial bulges in spiral galaxies supports the secular evolution hypothesis for the formation of the triaxial bulges in barred galaxies (Kormendy 1979; Pfenniger & Norman 1990) and the secular evolution of galaxies in general (Zhang 1996, 1998). There seems to be duty cycle of the bar for the secular evolution in the Hubble time.

## ACKNOWLEDGEMENTS

This work was supported in part by Pusan National University Grant and by the ARCSEC funded by KOSEF.

## REFERENCES

- Andredakis, Y. C., Peletier, R. F., & Balcells, M, 1995, The Shape of the Luminosity Profiles of Bulges of Spiral Galaxies, *MNRAS*, 275, 874
- Ann, H. B. 1995, Triaxial Bulges in Barred Galaxies, *JKAS*, 28, 209
- Ann, H. B. 2001, Hydrodynamic Simulations for the Nuclear Morphology of NGC 4314, *AJ*, 121, 2515
- Ann, H. B., & Lee, S.-W. 1987, Surface Photometry of Barred Galaxies: Global Structure of Barred Galaxies, *JKAS*, 20, 49
- Ann, H. B., & Lee, H. M. 2000, SPH Simulations of Barred Galaxies: Dynamical Evolution of Gaseous Disk, *JKAS*, 33, 1
- Baugh, C. M., Cole, S., & Frenk, C. S. 1996, Evolution of the Hubble Sequence in Hierarchical Models for Galaxy Formation, *MNRAS*, 283, 1361
- Benedict, G. F., Higdon, J. L., Tollestrup, E. V., Hahn, J., & Harvey, P. M. 1992, NGC 4314. I - Visible and short-wavelength infrared surface photometry of the nucleus and bar, *AJ*, 103, 757
- Benedict, G. F., Smith, B. L., & Kenney, J. D. P., 1996, NGC 4314. III. Inflowing Molecular Gas Feeding a Nuclear Ring of Star Formation, *AJ*, 112, 1318

- Carollo, C. M., Stiavelli, M., e Zeeuw, P. T., & Mack, J. 1997, *Spiral Galaxies with WFPC2.I.Nuclear Morphology, Bulges, Star Clusters, and Surface Brightness Profiles*, *AJ*, 114, 2363
- Courteau, S., de Jong, R. S., & Broeils, A. H. 1996, Evidence for Secular Evolution in Late-Type Spirals, *ApJ*, 457, L73
- Das, M., Teuben, P. J., Vogel, S. N., Regan, M. W., Sheth, K., Harris, A. I., & Jefferys, W. H. 2003, Central Mass Concentration and Bar Dissolution in Nearby Spiral Galaxies, *ApJ*, 582, 190
- Elmegreen, B. G. Elmegreen, D. M.1985, Properties of barred spiral galaxies, *ApJ*, 288, 438
- Elmegreen, B. G. 1999, Galactic Bulge Formation as a Maximum Intensity Starburst, *ApJ*, 517, 103
- Friedli, D., & Martinet, L. 1993, Bars Within Bars in Lenticular and Spiral Galaxies - a Step in Secular Evolution, *A&A*, 277, 27
- Friedli, D., & Benz, W. 1993, Secular evolution of isolated barred galaxies. I - Gravitational coupling between stellar bars and interstellar medium, *A&A*, 268, 65
- Friedli, D., & Benz, W. 1995, Secular evolution of isolated barred galaxies. II. Coupling between stars and interstellar medium via star formation, *A&A*, 301, 649
- Gnedin, N. Y., Norman, M. L., & Ostriker, J. P. 2000, Formation of galactic Bulges, *ApJ*, 540, 32
- Ichikawa, S.-I., Okamura, S., Watanabe, M., Hamabe, M., Aoki, T., & Kodaira, K. 1987, SPIRAL : surface photometry interactive reduction and analysis library. *Ann. Tokyo Astro. Obs. Tok.*, 21, 285
- Kauffmann, G., White, S. D. M., & Guiderdoni, B. 1993, The Formation and Evolution of Galaxies within Merging Dark Matter, *MNRAS*, 264, 201
- Kormendy, J. 1979, A morphological survey of bar, lens, and ring components in galaxies Secular evolution in galaxy structure, *ApJ*, 227, 714
- Kormendy, J. 1993, Kinematics Extragalactic Bulges: evidence that Some Bulges are really Disks, in *Galactic Bulges*, IAU Symposium 153, ed. H. J. Habing & H. B. Dejonghe (Kluwer, Dordrecht), p. 209
- Landolt, A. U. 1992, UBVRI photometric standard stars in the magnitude range 11.5-16.0 around the celestial equator, *AJ*, 104, 340
- Martini, P., & Pogge, R. W. 1999, Hubble Space Telescope Observations of the CFA Seyfert 2 Galaxies: The Fueling of Active Galactic Nuclei, *AJ*, 118, 2646
- Martini, P., Regan, M. W., Mulchaey, J. S., & Pogge, R. W. 2003, Circumnuclear Dust in Nearby Active and Inactive Galaxies. I. Data, *ApJS*, 146, 353
- Mulchaey, J., Regan, M. W., & Kundu, A. 1997, The Fueling of Nuclear Activity. I. A Near-Infrared Imaging Survey of Seyfert and Normal Galaxies, *ApJS*, 110, 299
- Navarro, J. F., Frenk, C. S., & White, S. D. M. 1995, The assembly of galaxies in a hierarchically clustering universe, *MNRAS*, 275, 56
- Noguchi, M. 1999, Early Evolution of Disk Galaxies: Formation of Bulges in Clumpy Young Galactic Disks, *ApJ*, 514, 77
- Noguchi, M. 2000, Secular Evolution of Late-type Galaxies: Formation of Bulges and the origin of Bar Dichotomy, *MNRAS*, 312, 194
- Norman, C. A., Sellwood, J. A., & Hasan, H. 1996, Bar Dissolution and Bulge Formation: an Example of Secular Dynamical Evolution in Galaxies, *ApJ*, 462, 114
- Pfenniger, D., & Norman, C. 1990, Dissipation in barred galaxies - The growth of bulges and central mass concentrations, *ApJ*, 363, 391
- Phillips, A. C., llingworth, G. D., MacKenty, J. W., & Franx, M. 1996, Nuclei of Nearby Disk Galaxies.I.A Hubble Space Telescope Imaging Survey, *AJ*, 111, 1566
- Pogge, R. W., & Martini, P. 2002, Hubble Space Telescope Imaging of the Circumnuclear Environments of the CFA Seyfert Galaxies: Nuclear Spirals and Fueling, *ApJ*, 569, 624
- Regan, M. W., & Mulchaey, J. 1999, Using HUBBLE SPACE TELESCOPE Imaging of Nuclear Dust Morphology to Rule Out Bars Fueling Seyfert Nuclei, *AJ*, 117, 2676
- Samland, M., & Gerhard, O. E. 2003, Samland, M.; Gerhard, O. E, *A&A*, 399,961
- Shaw, M. A., Axon, D., Probst, R., Gatley, I. 1995, Nuclear bars and blue nuclei within barred spiral galaxies, *MNRAS*, 274, 369
- Stark, A. A. 1977, Triaxial Models of the Bulge of M31, *ApJ*, 213, 368
- van den Bosch, F. C. 1998, The Formation of Disk-Bulge-Halo Systems and the Origin of the Hubble Sequence, *ApJ*, 507, 601
- Varela, A. M., Simonneau, E., & Munoz-Tunon, C. 1993, Triaxiality in the Bulge of Spirals: Dynamical Implications, in *Galactic Bulges*, IAU Symposium 153, ed. H. J. Habing & H. B. Dejonghe (Kluwer, Dordrecht), p. 435
- White, S. D. M., & Rees, M. K. 1978, Core condensation in heavy halos: a two-stage theory for galaxy formation and clustering, *MNRAS*, 183, 341
- Zhang, X. 1996, Secular Evolution of Spiral Galaxies. I. A Collective Dissipation Process, *ApJ*, 457, 125
- Zhang, X. 1998, Secular Evolution of Spiral Galaxies. II. Formation of Quasi-stationary Spiral Modes *ApJ*, 499, 93